Krypton-81 dating constrains timing of deep groundwater flow activation 2 3 Ji-Hyun Kim¹, Grant Ferguson^{1,2}, Mark Person³, Wei Jiang⁴, Zheng-Tian Lu⁴, Florian Ritterbusch⁴, Guo-4 Min Yang⁴, Rebecca Tyne^{5*}, Lydia Bailey⁶, Chris Ballentine⁵, Peter Reiners⁶, Jennifer McIntosh^{1, 2} 5 6 7 ¹Department of Hydrology and Atmospheric Sciences, University of Arizona, Tucson, AZ, USA 8 ² Department of Civil, Geological and Environmental Engineering, University of Saskatchewan, 9 Saskatoon, Canada ³ Department of Earth and Environmental Science, New Mexico Tech, Socorro, NM, USA 10 11 ⁴ School of Physics, University of Science and Technology of China, 96 Jinzhai Road, Hefei 230026, 12 China ⁵ Department of Earth Sciences, University of Oxford, Oxford, England, UK 13 ⁶ Department of Geosciences, University of Arizona, Tucson, AZ, USA 14 15

* Rebecca Tyne is now affiliated with the Woods Hole Oceanographic Institution.

1

16

17

Geophysical Research Letters

18 CRediT

- Ji-Hyun Kim: Investigation Data collection; conceptualization; methodology; visualization;
- 20 writing original draft
- Grant Ferguson: Conceptualization; methodology; visualization; writing review & editing
- Mark Person: conceptualization; writing review & editing
- Wei Jiang: Formal analysis of ⁸¹Kr; methodology; writing review & editing
- Zheng-Tian Lu: Formal analysis of ⁸¹Kr; methodology
- Florian Ritterbusch: Formal analysis of ⁸¹Kr; methodology; writing review & editing
- Guo-Min Yang: Formal analysis of ⁸¹Kr; methodology
- Rebecca L. Tyne: validation; writing review & editing
- Bailey: Geological conceptualization
- Chris J. Ballentine: validation
- Peter W. Reiners: Geological conceptualization; writing review & editing
- Jennifer McIntosh: Conceptualization; project development; supervision; writing review &
- 32 editing

Key points

33

- Meteoric waters up to 3 km in basinal aquifers are <1.1 Ma.
- Recent, rapid denudation of the Colorado Plateau enabled deep circulation of meteoric water and flushing of connate brines.
- Krypton-81 dating can illuminate the timescales and extent of meteoric circulation in response to
 geologic and/or climatic forcings.

Abstract

Krypton-81 dating provides new insights into the timing, mechanisms, and extent of meteoric flushing versus retention of saline fluids in the subsurface in response to changes in geologic and/or climatic forcings over 50 ka to 1.2 Ma year timescales. Remnant Paleozoic seawater-derived brines associated with evaporites in the Paradox Basin, Colorado Plateau, are beyond the ⁸¹Kr dating range (>1.2 Ma) and have likely been preserved due to negative fluid buoyancy and low permeability. ⁸¹Kr dating of formation waters above the evaporites indicates topographically-driven meteoric recharge and salt dissolution since the Late Pleistocene (0.03-0.8 Ma). Formation waters below the evaporites (up to 3 km depth), in basal aquifers, contain relatively young meteoric water components (0.4-1.1 Ma based on ⁸¹Kr) that partially flushed remnant brines and dissolved evaporites. We demonstrate that recent, rapid denudation of the Colorado Plateau (<4-10 Ma) activated deep, basinal-scale flow systems as recorded in ⁸¹Kr groundwater age distributions.

Plain language summary

Landscape changes over geological time alter hydraulic gradients and the presence or absence of near-surface confining units, which drive the evolution of subsurface flow systems. However, our understanding of the time required for groundwater flow systems to respond to geological processes, such as shifts in topography, stratigraphy, and permeability structures, is still limited. This study uses krypton-81 dating to constrain the age of meteoric waters in the Paradox Basin in the Colorado Plateau and constrain the timing of groundwater recharge into basinal aquifers. We discovered that rapid, widespread erosion and incision in the Colorado Plateau in the last 10 Ma activated deep meteoric circulation, partially flushing residual ancient seawater-derived brines from aquifers above and below thick, evaporite confining units and dissolving salt. Krypton-81 dating may provide insights into timescales and drivers of subsurface fluid flow and connectivity with the near-surface in other environments.

1. Introduction

Constraining the dynamic interface between circulating meteoric waters and deeper more stagnant saline fluids is important for groundwater supplies (Kang and Jackson, 2016; Ferguson, McIntosh, Perrone et al., 2018), mineral resources (Sanford, 1994; Garven, 1995), energy extraction and storage (Garven, 1989; Spangler et al., 1996; Zheng et al., 2012), isolation of anthropogenic waste products (Cherry et al., 2014; Sturchio et al., 2014; Ferguson, McIntosh, Perrone et al., 2018), and subsurface microbial life (Warr et al., 2018; Lollar et al., 2021). Circulating meteoric waters, present in the upper few kilometers of the Earth's crust (McIntosh and Ferguson, 2021), transport an appreciable mass of fluids and solutes on timescales of tens of years to ka to Ma (Castro et al., 1998; Lehmann et al., 2003; Zhou et al., 2005; Schlegel et al., 2011; Aggarwal et al., 2015; Gerber et al., 2017; Jasechko et al., 2017). Remnant Paleozoic age (>250 Ma) seawater is present at depth and in the interior of sedimentary basins often associated with evaporite deposits (Carpenter, 1978; Hanor, 1994; Lehmann et al., 2003; Ma et al., 2009; Kharaka and Hanor, 2014), while even older saline fluids (>1 Ga) are trapped within isolated fracture systems in crystalline basement rocks (Holland et al. 2013; Warr et al., 2018).

The depth of meteoric circulation and interface with more stagnant saline fluids has evolved over geologic time in response to changes in topography, stratigraphy, and permeability (Bethke and Marshak, 1990; Lazear et al., 2013; Yager et al., 2017; Ferguson, McIntosh, Grasby et al., 2018; Chaudhary et al., 2019). For example, past orogenic events drove ore-forming brines (e.g., Wisconsin and Illinois basins; Bethke and Marshak, 1990) and hydrocarbons to distal margins of basins (e.g., Western Canada Sedimentary Basin; Garven, 1989). Pleistocene continental glaciation enhanced the depth of meteoric circulation by increasing hydraulic heads at the ground surface (Person et al., 2007). Low permeability layers can impede meteoric infiltration, reduce flow rates, and control response times of flow systems to changes in driving forces (Neuzil, 1986; Tóth, 1999) and their removal can increase circulation rates.

Basinal brines can be brought close to the surface by denudation (Yager et al., 2017). High-relief

landscapes of sedimentary basins in western North America were shaped by erosion and incision along rivers during the Laramide Orogeny (e.g., Permian Basin; Chaudhary et al., 2019; Grand Mesa; Aslan et al., 2019) or during the Neogene period (e.g., denudation of Colorado Plateau; Lazear et al., 2013). This erosion and incision would have increased hydraulic gradients, breached or removed aquitards, while denudation would have brought deeper strata closer to the surface.

The depth of circulation of meteoric waters is a function of the hydraulic head (e.g., topography) available to drive regional groundwater flow and the tendency for saline fluids at depth to stagnate due to negative buoyancy (Ferguson, McIntosh, Grasby et al., 2018; McIntosh and Ferguson, 2021). The driving force ratio (DFR) compares these two forces (Bachu, 1995; Ferguson, McIntosh, Grasby et al., 2018). If a basin has a DFR greater than 1, trapping of high-density residual brines would be expected. Conversely, if a basin has a DFR less than 1, residual brines may be flushed by regional groundwater flow (Ferguson, McIntosh, Grasby et al., 2018). Most sedimentary basins containing evaporated paleo-seawater (EPS) have DFR >1, for example in the Permian, Illinois, Appalachian, and Michigan basins (Ferguson, McIntosh, Grasby et al., 2018).

Interestingly, the Paradox Basin in the Colorado Plateau has a low DFR (<1; Ferguson, McIntosh, Grasby et al., 2018) based on relatively high modern relief, suggesting that saline fluids within the basin should have been flushed by topographically-driven regional groundwater flow. Yet, EPS is present at depth within extensive Pennsylvanian marine evaporite confining units and, to a lesser extent, in the overand under-lying aquifer systems (Kim et al., 2022). We hypothesize that recent denudation of the Colorado Plateau and deep incision of the Colorado River (<4-10 Ma) created high topographic gradients that led to partial flushing of remnant saline fluids (e.g., EPS), while EPS is retained within evaporites due to their low permeability and relatively short timescales of flushing. To test this hypothesis, we applied ⁸¹Kr dating to provide constraints on the timescales and extent of meteoric water circulation vs. retention of connate brines in the Paradox Basin.

⁸¹Kr is derived solely from atmospheric sources produced by cosmic rays with negligible subsurface production (Collon et al., 2004; Sturchio et al., 2014), unlike more traditional tracers, such as ⁴He or ³⁶Cl (Ballentine and Burnard, 2002; Phillips, 2000), and can date groundwater from ~40 ka to 1.2 Ma (half-life 229,000 years; Loosli and Oeschger, 1969) beyond the range of radiocarbon. Recent advances in Atom Trap Trace Analysis (ATTA) (Jiang et al., 2012 & 2020; Lu et al., 2014) which has reduced sample size alongside the development of gas extraction devices for field sampling (Yokochi, 2016; Jiang et al., 2020) have enabled the application of ⁸¹Kr as an age tracer of subsurface flow systems (Aggarwal et al., 2015; Matsumoto et al., 2018 & 2020; Ram et al., 2021). ⁸⁵Kr (10.7-year half-life), which is present in the modern atmosphere, has been used as an indicator for modern air contamination (Sturchio et al., 2014; Yokochi et al., 2019).

Most ⁸¹Kr studies to date have been in confined fresh to brackish aquifer systems (Lehmann et al., 2003; Sturchio et al., 2004; Matsumoto et al., 2018; Yechieli et al., 2019; Yokochi et al., 2019). Sturchio et al. (2014) applied ⁸¹Kr to date saline meteoric groundwater (~130 and ~330 ka) in carbonates overlying evaporites at the Waste Isolation Pilot Plant, New Mexico. In the Baltic Artesian Basin, ⁸¹Kr dating of groundwater from the basal, saline aquifer system identified three distinct fluid components (300 ka to >1.2 Ma) with Pleistocene glaciation suppressing the interface between meteoric water and basinal brines (Gerber et al., 2017). These past studies have focused on using ⁸¹Kr to examine changes in groundwater systems due to shifts in climate during the Pleistocene Epoch. Here, we measure ⁸¹Kr in fresh to saline fluids to investigate the effects of geological processes, such as denudation and incision, on activation of deep meteoric flow systems. In addition, we combine ⁸¹Kr ages with geochemical results to estimate the age distribution of meteoric water components of the basinal fluids.

2. Study Site

The Paradox Basin, in the Colorado Plateau, is a foreland basin (Barbeau, 2003) located in Utah and Colorado, USA (Fig. 1a), underlain by Precambrian basement rocks (Bremkamp and Harr, 1988). The basal sedimentary units are comprised of Cambrian, Devonian (e.g., McCracken Sandstone (Ss) member of Elbert Formation (Fm)), and Mississippian (e.g., Leadville Limestone (Ls)) formations deposited in marine environments (Fig. 1c). During the Pennsylvanian, marine evaporites were cyclically deposited with interbedded black shales, comprising the Paradox Fm (up to 2.5 km thick) (Fig. 1c; Hite et al., 1984). Examples of members of Paradox Fm are the Ismay-Desert Creek carbonate and Cane Creek shale. Overlying the Paradox Fm evaporites, the Pennsylvanian Honaker Trail Fm contains eolian and fluvial beds. Thick deposition of Permian (e.g., Cutler Fm), Jurassic (e.g., Navajo Ss), Cretaceous (e.g., Burro Canyon Fm), and Tertiary sediments, from erosion of Precambrian rocks in the Uncompahgre Uplift, led to plastic flow of the evaporites and formation of salt anticlines and associated faults along the northeastern side of the basin (Fig. 1b). The Mancos Shale was deposited in the Western Interior Cretaceous seaway within the upper hydrostratigraphic unit as a regional confining unit. Intrusion of laccoliths such as the Abajo and La Sal mountains occurred during the Tertiary (28 Ma; Nuccio and Condon, 1996).

Relatively recently, rapid denudation of the Colorado Plateau and deep incision of the Colorado River within <4-6 Ma (Murray et al., 2019) or <10 Ma (Karlstrom et al., 2012; Lazear et al., 2013; Pederson et al., 2013) created steep topographic gradients and likely led to widespread paleofluid flow events (Garcia et al., 2018; Bailey et al., 2021). The maximum net eroded sediment thickness, derived from subtraction of the modern topographic surface from the paleosurface, is about 1-3 km within the past 10 Ma across the Paradox Basin (Lazear et al., 2013). For example, the Leadville Ls would have reached a depth of ~5000 m during maximum burial (Nuccio and Condon, 1996), compared to only ~2000 m today. Since the denudation of Colorado Plateau, most of the Mancos Shale has been eroded within the Paradox Basin, except in the Book Cliffs area and southwestern Colorado (Molenaar, 1981).

The Paradox and Lower Honaker Trail formations form a regional confining unit (middle hydrostratigraphic unit) that separates aquifer systems in the upper and lower hydrostratigraphic units (Fig. 1c; Hanshaw and Hill, 1969; Thackston et al., 1981). Beneath the Paradox Fm, the Mississippian through Devonian formations comprise a single, lower hydrostratigraphic unit, or basal aquifer system, with regional groundwater flow towards the southwest and with local recharge around laccoliths or along the margins of the salt anticlines. In the upper hydrostratigraphic unit above the Paradox Fm, groundwater flow is mainly controlled by local topography with recharge around salt anticlines, uplifts, and mountains.

3. Methods

To constrain the ⁸¹Kr ages of formation waters, a total of 13 dissolved and produced gas samples were collected for krypton isotopes in 2018 and 2020 from near surface (<500 m depth) to basal geologic formations (up to 2.7 km depth). The location and geologic formation of samples are displayed in Figure 1a & 1c and Table S1. Nine gas samples were collected directly from oil and gas producing wells. Three gas samples were extracted from fresh to brackish groundwater monitoring wells and one gas sample was extracted from a lithium exploration well completed in the Cane Creek member of the Paradox Fm. One modern air sample was collected to measure ⁸⁵Kr in the atmosphere, so that possible contamination with modern air in the samples can be quantified and corrected. The gas samples were collected into aluminum gas tanks attached to the wellhead through a pressure regulator. In case of groundwater wells, a hydrophobic membrane was used to extract dissolved gas from water and convey the extracted gas to evacuated tanks (Yokochi, 2016; Jiang et al., 2020). Kr separation from the gases and the ⁸¹Kr analysis, using Atom Trap Trace Analysis (ATTA), were performed at the University of Science and Technology of China (Dong et al., 2019; Jiang et al., 2012 & 2020). Detailed methods for sampling and analysis are described in Text S1. ⁸¹Kr results were paired with previously published hydrochemical data (Kim et al., 2022), from corresponding water samples from the same wells (where available) or the same fields where

the gas samples were collected (Table S2). The hydrochemical data were used to calculate the extent of meteoric recharge, salt dissolution, and mixing with remnant EPS-derived brines. Only ⁸¹Kr data for the Permian Cutler Fm from the Andy's Mesa gas field were compared with available water data from a different field (Greater Aneth oil field; Spangler et al., 1996). ⁸⁵Kr was also analyzed to identify and correct for air contamination during sampling (Jiang et al., 2012).

Hydrochemical data, including Na/Cl, Cl/Br, and δD_{water} were compiled from previously published sources (Hanshaw and Hill, 1969; Blondes et al., 2018; Kim et al., 2022) to calculate the extent of meteoric recharge, salt dissolution, and mixing with remnant EPS-derived brines.

The DFR was used to evaluate the mobility (e.g., flushing or retention) of saline fluids in the Paradox Basin over geologic time. The DFR is calculated by comparing the force due to pressure and topographic differences to drive regional groundwater flow to the force due to negative buoyancy acting on saline fluids (Ferguson, McIntosh, Grasby et al., 2018; McIntosh and Ferguson, 2021):

$$DFR = \left(\frac{\Delta \rho}{\rho_0}\right) \frac{|\nabla E|}{|\nabla H_0|_h}$$

where $\Delta \rho$ is the difference between fluid density and reference density; ρ_0 is reference density; ∇H_0 is the gradient of equivalent freshwater head; ∇E is the structural gradient of the groundwater flow system. Here, DFR values for each formation water sampled in the Paradox Basin were estimated at different time periods using estimates of past topographic gradients, assuming consistent fluid density as described in section 7.

4. Widespread Meteoric Circulation

Formation waters with molar Na/Cl ~1 across the Paradox Basin, in upper and lower hydrostratigraphic units, indicate widespread influx of meteoric waters (initially undersaturated with respect to halite) and dissolution of halite associated with the Paradox Fm evaporites (Fig. 1a). High

molar Cl/Br of formation waters, found at shallow depth (≤15 m) above salt anticlines ("salt anticline brine") and beneath the evaporites (e.g., Leadville Ls brine), also indicate dissolution of the evaporites by meteoric circulation (Fig. 2b).

In addition to the salt dissolution-derived brines, EPS within the Paradox Fm, represented by a brine sample from the Cane Creek member ("Cane Creek brine"), is another major source of salinity in the formation waters of the Paradox Basin and has a distinct geochemical and isotopic signature with low Na/Cl (0.2), Na/Br (28), and Cl/Br (156) molar ratios relative to modern seawater (0.85, 565, and 659, respectively) and the highest $\delta^{18}O_{water}$ and δD_{water} values, plotting to the right of the Local Meteoric Water Line (Table S2; Kim et al., 2022). δD_{water} values (Fig. 2b-c; Table S2) show the variable amount of mixing between meteoric water recharge and remnant EPS for each formation water.

The salt anticline brines and Burro Canyon Fm brackish groundwater have low δD_{water} values and 14 C ages consistent with Holocene to Pleistocene recharge (Noyes et al., 2021) with almost 100% meteoric water, while deep basinal brines (Honaker Trail Fm, Desert Creek, Leadville Ls, and McCracken Ss) consist of varied proportions of meteoric water and EPS (Fig. 2b-c). For example, the Leadville Ls brine contains ~74 % meteoric water and ~26 % EPS based on δD_{water} values. This is somewhat consistent with PHREEQC inverse mixing model results using major ion chemistry indicating 96 % meteoric water and 4 % EPS in the Leadville Ls brine sample (Kim et al., 2022). Both results are in qualitative agreement with the high proportion of meteoric waters in the lower hydrostratigraphic unit, dilution of connate saline fluids, and regeneration of salinity via salt dissolution.

5. Meteoric Flushing vs. Retention of Evaporated Paleo-Seawater-Derived Brine

Fresh to brackish shallow groundwater from the Cretaceous Burro Canyon Fm and Jurassic Navajo Ss are younger than 15-35 ka based on ⁸¹Kr (>90 percent modern krypton, pMKr), indicating meteoric circulation and subsequent salt dissolution since at least the Late Pleistocene (Fig. 2a). The ⁸¹Kr

age results (16-35 ka and <23 ka) of groundwater in the Navajo Ss aquifer are consistent with corrected ¹⁴C age results (36 and 25 ka, respectively) of the same groundwater wells from a previous study (Noyes et al., 2021). In the deeper brines, the ⁸¹Kr age of formation waters in the Cutler and Honaker Trail formations and Desert Creek member of the Paradox Fm are ~890 ka, 530-754 ka, and 600 ka - 1.2 Ma with detectable ⁸¹Kr (>2.5 pMKr), respectively, suggesting that the meteoric components of fluids in the upper hydrostratigraphic unit are younger than 1.2 Ma (Fig. 2a).

The Cane Creek brine from the Paradox Fm evaporite has too much uncertainty to correct for 81 Kr (Table S2). Given the chemical and isotopic signatures indicative of Paleozoic EPS (i.e., Cl/Br << 659, Na/Cl << 0.85, δ^{18} O ~5‰), the Cane Creek brine is likely the oldest, beyond the 81 Kr dating limit (>1.2 Ma, Fig. 2a), and has the same 81 Kr as the underlying oldest formation water with <2.5 pMKr in the lower hydrostratigraphic unit. The low permeability of the Paradox Fm evaporites likely enabled retention of these paleofluids and prevented influx of meteoric waters (Gloyna and Reynolds, 1961; Neuzil, 1986).

Formation waters in the lower hydrostratigraphic unit contain variable ⁸¹Kr from <2.5 to 9.1 pMKr (Fig. 2a; Table S2). The ⁸¹Kr ages of the formation waters with detectable ⁸¹Kr range from 790 to 878 ka, indicating the presence of meteoric waters in the basal aquifers, which is consistent with Cl/Br and δD_{water} results of Leadville Ls brine (Fig. 2b), and relatively recent circulation of meteoric water. The ⁸¹Kr ages of the formation waters beyond the ⁸¹Kr dating limit suggest the presence of residual EPS in the basal aquifers due to preservation, dispersive processes or as the result of diffusion from the overlying Paradox Fm. We hypothesize that relatively young meteoric water diluted the EPS-derived brines and dissolved halite resulting in salt dissolution-derived brines.

6. Timing of meteoric water recharge into formation above/below Paradox Fm

A simple binary mixing model using the measured 81 Kr and δD_{water} of formation waters was constructed to calculate the estimated age of meteoric water components of each formation water and better constrain the timing of meteoric recharge (Fig. 2c). The binary mixing model accounts for the proportion of 81 Kr abundances between two endmembers: 1) meteoric water with different 81 Kr (age) for each formation water and 2) EPS with consistent low 81 Kr abundance. The proportion of the two endmembers for each formation water was based on δD_{water} values of fluids (Fig. 2b). δD_{water} was used in this study rather than $\delta^{18}O_{water}$, as more samples were included in a mixing space consisting of the two endmembers with δD_{water} and other parameters (CI/Br or 81 Kr). The δD_{water} value of the initial meteoric water endmember was assumed to be the average of the fresh-brackish groundwater samples (PW-8, PW-11, and PW-12; -106.8 ‰), which had an average 81 Kr abundance of ~100 pMKr indicating meteoric water in contact with the atmosphere. The uncertainty for different δD_{water} values of the initial meteoric water endmember possibly impacts the proportion and age of meteoric water components (as shown in the crosshairs in Fig. 2c). The saline fluid endmember was represented by EPS with an assumed 81 Kr value (2.5 pMKr) from the underlying oldest formation waters (Leadville Ls brine) and measured δD_{water} (-7.57 ‰) values from the Cane Creek brine.

In the Lisbon Valley area, in the northeastern part of the basin (Fig. 1a), formation waters in the Honaker Trail Fm consist of 40-55 % meteoric water with an 81 Kr age of 245-595 ka and 45-60 % EPS (Fig. 2c). Formation waters in the Leadville Ls and McCracken Ss are composed of 28-52 % meteoric water with an 81 Kr age of 440 ka - 1.1 Ma and 48-72 % EPS. The lower hydrostratigraphic unit shows an older and wider range of meteoric components than the upper hydrostratigraphic unit, indicating deep circulation of meteoric water into the basal aquifer system in the Lisbon Valley area was activated as early as \sim 1.1 Ma. However, the averaged δD_{water} value from different wells than the 81 Kr data in the same field (Table S2) can over- or under-estimate the proportion and age of meteoric water component in the formation water.

Formation waters in the Cutler Fm in the Andy's Mesa field in the northeastern parts of the basin (Fig. 1a) contain a large component (93 %) of older (872 ka) meteoric water, compared to the meteoric water component of formation waters in the underlying Honaker Trail Fm from the Lisbon Valley (Fig. 2c). It is possible that meteoric water circulation was activated earlier in the Cutler Fm with limited fracture connectivity between formations (Anna et al., 2014). However, because the δD values used for the Cutler Fm came from a different field (Greater Aneth oil field; Spangler et al., 1996) than the ⁸¹Kr data, the percent meteoric water may have been over- or under-estimated.

In the Greater Aneth oil field located along the southwestern margin of the Paradox Basin (Fig. 1a), meteoric water components for formation waters in the Desert Creek member of the Paradox Fm are lower in proportion (28 %) and relatively young (195-215 ka), compared to over- and under-lying formations in other parts of the basin (Fig. 2c). The differences in the extent and timing of meteoric recharge may be explained by differences in the local permeability structure, depth, and topography. The Paradox Fm in the Greater Aneth oil field contains fewer evaporites deposited in the carbonate shelf and is located at relatively shallow depths (≤1.8 km; Spangler et al., 1996), which may have enabled influx of meteoric water into the Paradox Fm.

7. The evolution of meteoric circulation

In order to constrain the evolution of meteoric circulation over geologic time, it is necessary to understand the past topography and burial history including denudation and incision events. Prior to widespread erosion of the Mancos Shale and overlying units, underlying formation waters were deeply buried. The basin before 10 Ma (Fig. 3a) was covered by ~1300 m of additional sediments (Nuccio and Condon, 1996). Furthermore, considering the incision rate of 126 m/Ma (Darling et al., 2012), the elevation of the regional discharge was also 1260 m higher (Fig. 3a) compared to the modern topography (Fig. 3b). The combination of lower topographic relief and lower permeability strata in the past would

have resulted in a water table that closely followed topography (Haitjema and Mitchell-Brucker, 2006: Gleeson et al., 2011), resulting in lower regional hydraulic gradients. The saline fluids (e.g., EPS) may have been expelled very slowly (red arrow in Fig. 3a) due to compaction (Bethke and Marshak, 1990), compared to the shallow regional flow system (blue arrow in Fig. 3a). Because of a higher ratio of the structural gradient of the groundwater flow system (∇E) to equivalent freshwater head gradient (∇h) before 10 Ma, DFR values for deeper formations were likely much higher than 1 (Fig. 3c), indicating the retention of most of saline fluids. Furthermore, brine densities before meteoric influx were likely higher than they are today, resulting in even stronger tendency to retain with higher DFR values before 10 Ma.

Following widespread erosion of Mancos Shale and other units from 10 Ma and incision of rivers (Fig. 3b), the modern water table with elevations as high as 2500 masl near the La Sal Mountains and regional discharge areas of ~1100 masl along the Colorado and San Juan rivers shows DFR <1, indicating active circulation of meteoric water throughout the basin (Fig. 3c). The deep meteoric circulation would have flushed residual saline fluids in aquifers above and below the evaporite (Fig. 3b). Internal drains within the basin (e.g., Dolores River in the Paradox Valley or Salt Creek in the Sinbad Valley) would show higher DFR values due to their higher elevation than regional discharge areas, yet their sufficient high head gradients from the La Sal mountains still enable circulation of meteoric water below the Paradox Fm. The rate and depth of circulation of meteoric water would have increased as incision of the Colorado Plateau created lower elevation discharge points over time. The lack of waters beyond the ⁸¹Kr ages with meteoric components suggests that although incision of the Colorado Plateau began 4 -10 Ma (Lazear et al., 2013; Murray et al., 2019), there was insufficient incision to activate regional groundwater flow in the deeper parts of the Paradox Basin until ~1 Ma.

Changes in topography, stratigraphy, and permeability structures due to denudation would have increased hydraulic gradients, removed low permeability layers, or brought deeper strata closer to the surface, which enhance the extent and rate of meteoric circulation and deeper interface with stagnant saline fluids. Increases in meteoric circulation depth has also been observed in other sedimentary basins in

the southwestern US, such as the Permian (Engle et al., 2016; Chaudhary et al., 2019), Uinta (Zhang et al., 2009) and San Juan (Scott et al., 1994) basins, that have been affected by denudation. The role of landscape evolution over the last few million-years on the timing and extent of recent deep meteoric circulation (<1.2 Ma) through subsurface flow systems could be further tested by ⁸¹Kr dating of basinal fluids.

8. Conclusions

This study showed that ⁸¹Kr is an effective tool to illuminate the timescales and extent of meteoric flushing vs. retention of brines in sedimentary basins. The application of ⁸¹Kr combined with δD_{water} to examine the meteoric component of saline fluids in the Paradox Basin revealed deep meteoric circulation as early as 1.1 Ma. Rapid denudation enhanced topographic gradients and altered the permeability structure (i.e., erosion of shale confining units) enabling deep circulation of meteoric water and partial flushing of basal aquifers, while evaporated paleo-seawater (>1.2 Ma) is still retained within the evaporite confining unit.

Our results demonstrate that ⁸¹Kr can be used to provide insights into the evolution of groundwater flow systems due to geological processes operating on times scales of up to ~1 Ma. The shift from a static to dynamic view of geology that this helps to facilitate is necessary as we seek to understand how groundwater flow systems have changed over geologic time and what effects this may have on geochemical cycles and subsurface life, and energy extraction, storage, and waste isolation.

Open Research

Kr, Na, Cl, Br, and δD_{water} data is stored and publicly available on Hydroshare (at:

http://www.hydroshare.org/resource/d2a724a994b34fa3880ca21562912788). Hydrochemical data (Na,

- Cl, Br, and δD_{water}) are available through Hanshaw and Hill (1969), Spangler et al. (1996), Blondes et al.
- 349 (2018), and Kim et al. (2022). ¹⁴C data are available through Noyes et al. (2021).

350

351

Acknowledgement

- Funding for this research was provided by the W.M. Keck Foundation, CIFAR, NSF EAR (#2120733),
- National Key Research and Development Program of China (Grant No. 2016YFA0302200), and National
- Natural Science Foundation of China (Grants No. 41727901). McIntosh and Ballentine are fellows of the
- 355 CIFAR Earth4D Subsurface Science and Exploration program. The authors would like to acknowledge
- the U.S. Bureau of Reclamation, Paradox Resources, Navajo Petroleum, Anson Resources, and Lantz
- 357 Indergard (Lisbon Valley Mining Co.), Chandler Noyes and Ambria Dell'Oro for help with sampling.
- 358 Drs. Isabel Barton, Mark Barton, Steven Lingrey, and Bob Krantz provided insights on stratigraphy and
- topography in the Paradox Basin. The authors also would like to acknowledge the reviewers for their
- 360 comments that significantly improved the manuscript.

361

362

References

- 363 Aggarwal, P. K., Matsumoto, T., Sturchio, N. C., Chang, H. K., Gastmans, D., Araguas-Araguas, L. J., ...
- & Torgersen, T. (2015). Continental degassing of 4 He by surficial discharge of deep groundwater.
- 365 Nature Geoscience, 8(1), 35-39.
- Anna, L. O., Whidden, K. J., & Pearson, K. M. (2014). Assessment of Continuous Oil and Gas
- Reservoirs, Paradox Basin, Utah, Colorado, New Mexico, and Arizona.
- Aslan, A., Karlstrom, K. E., Kirby, E., Heizler, M. T., Granger, D. E., Feathers, J. K., ... & Mahan, S. A.
- 369 (2019). Resolving time-space histories of Late Cenozoic bedrock incision along the Upper Colorado
- 370 River, USA. Geomorphology, 347, 106855.
- Baars, D. L., 1966, Pre-Pennsylvanian paleotectonics—Key to basin evolution and petroleum occurrences
- in Paradox Basin, Utah and Colorado: American Association of Petroleum Geologists Bulletin, v. 50, no.
- 373 10, p. 2082-2111.

- Bachu, S. (1995). Flow of variable-density formation water in deep sloping aquifers: review of methods
- of representation with case studies. Journal of Hydrology, 164(1-4), 19-38.
- Bailey, L. R., Kirk, J., Hemming, S. R., Krantz, R. W., & Reiners, P. W. (2021). Eocene fault-controlled
- fluid flow and mineralization in the Paradox Basin, United States. Geology.
- Ballentine, C. J., & Burnard, P. G. (2002). Production, release and transport of noble gases in the
- continental crust. Reviews in mineralogy and geochemistry, 47(1), 481-538.
- Barbeau, D. L. (2003). A flexural model for the Paradox Basin: implications for the tectonics of the
- Ancestral Rocky Mountains. Basin Research, 15(1), 97-115.
- Bethke, C. M., & Marshak, S. (1990). Brine migrations across North America—The plate tectonics of
- groundwater. Annual Review of Earth and Planetary Sciences, 18(1), 287-315.
- Blondes, M. S., Gans, K. D., Engle, M. A., Kharaka, Y. K., Reidy, M. E., Saraswathula, V., Thordsen, J.
- J., Rowan, E. L., & Morrissey, E. A. (2018) U.S. Geological Survey National Produced Waters
- Geochemical Database: U.S. Geological Survey data release, ver. 2.3, January.
- 387 https://doi.org/10.5066/F7J964W8
- Bremkamp, W., & Harr, C. L. (1988). Area of least resistance to fluid movement and pressure rise.
- Paradox Valley Unit, Salt Brine Injection Project, Bedrock, Colorado, a report prepared for the US
- 390 Bureau of Reclamation, Denver, Colorado, 39.
- 391 Carpenter, A. B. (1978). Origin and chemical evolution of brines in sedimentary basins. In SPE Annual
- Fall Technical Conference and Exhibition. Society of Petroleum Engineers.
- Castro, M. C., Goblet, P., Ledoux, E., Violette, S., & de Marsily, G. (1998). Noble gases as natural tracers
- of water circulation in the Paris Basin: 2. Calibration of a groundwater flow model using noble gas
- isotope data. Water Resources Research, 34(10), 2467-2483.
- Castro, M. C., Jambon, A., De Marsily, G., & Schlosser, P. (1998). Noble gases as natural tracers of water
- 397 circulation in the Paris Basin: 1. Measurements and discussion of their origin and mechanisms of vertical
- transport in the basin. Water Resources Research, 34(10), 2443-2466.
- Chaudhary, B. K., Sabie, R., Engle, M. A., Xu, P., Willman, S., & Carroll, K. C. (2019). Spatial
- 400 variability of produced-water quality and alternative-source water analysis applied to the Permian Basin,
- 401 USA. Hydrogeology Journal, 27(8), 2889-2905.
- 402 Cherry, J. A., Alley, W. M., & Parker, B. L. (2014). Geologic Disposal of Spent Nuclear Fuel. The Bridge
- on Emerging Issues in Earth Resources Engineering, 44(1), 51-59.
- Collon, P., Kutschera, W., & Lu, Z. T. (2004). Tracing noble gas radionuclides in the environment. Annu.
- 405 Rev. Nucl. Part. Sci., 54, 39-67.
- Darling, A. L., Karlstrom, K. E., Granger, D. E., Aslan, A., Kirby, E., Ouimet, W. B., ... & Cole, R. D.
- 407 (2012). New incision rates along the Colorado River system based on cosmogenic burial dating of
- 408 terraces: Implications for regional controls on Quaternary incision. Geosphere, 8(5), 1020-1041.
- 409 Dong, X. Z., Ritterbusch, F., Chu, Y. Q., Gu, J. Q., Hu, S. M., Jiang, W., ... & Zhao, L. (2019). Dual
- 410 separation of krypton and argon from environmental samples for radioisotope dating. Analytical
- 411 chemistry, 91(21), 13576-13581.

- 412 Engle, M. A., Reyes, F. R., Varonka, M. S., Orem, W. H., Ma, L., Ianno, A. J., ... & Carroll, K. C. (2016).
- 413 Geochemistry of formation waters from the Wolfcamp and "Cline" shales: Insights into brine origin,
- reservoir connectivity, and fluid flow in the Permian Basin, USA. Chemical Geology, 425, 76-92.
- 415 Ferguson, G., McIntosh, J. C., Grasby, S. E., Hendry, M. J., Jasechko, S., Lindsay, M. B., & Luijendijk,
- E. (2018). The persistence of brines in sedimentary basins. Geophysical Research Letters, 45(10), 4851-
- 417 4858.
- 418 Ferguson, G., McIntosh, J. C., Perrone, D., & Jasechko, S. (2018). Competition for shrinking window of
- low salinity groundwater. Environmental Research Letters, 13(11), 114013.
- Garcia, V. H., Reiners, P. W., Shuster, D. L., Idleman, B., & Zeitler, P. K. (2018). Thermochronology of
- 421 sandstone-hosted secondary Fe-and Mn-oxides near Moab, Utah: Record of paleo-fluid flow along a
- 422 fault. GSA Bulletin, 130(1-2), 93-113.
- 423 Garven, G. (1989). A hydrogeologic model for the formation of the giant oil sands deposits of the
- Western Canada sedimentary basin. American Journal of Science, 289(2), 105-166.
- 425 Garven, G. (1995). Continental-scale groundwater flow and geologic processes. Annual Review of Earth
- 426 and Planetary Sciences, 23(1), 89-117.
- Gerber, C., Vaikmäe, R., Aeschbach, W., Babre, A., Jiang, W., Leuenberger, M., ... & Purtschert, R.
- 428 (2017). Using 81Kr and noble gases to characterize and date groundwater and brines in the Baltic
- 429 Artesian Basin on the one-million-year timescale. Geochimica et Cosmochimica Acta, 205, 187-210.
- Gleeson, T., Marklund, L., Smith, L., & Manning, A. H. (2011). Classifying the water table at regional to
- continental scales. Geophysical Research Letters, 38(5).
- Gloyna, E. F., & Reynolds, T. D. (1961). Permeability measurements of rock salt. Journal of geophysical
- 433 research, 66(11), 3913-3921.
- Hanor, J. S. (1994). Physical and chemical controls on the composition of waters in sedimentary basins.
- 435 Marine and petroleum geology, 11(1), 31-45.
- Hanshaw B. B., and Hill G. A., 1969, Geochemistry and hydrodynamics of the Paradox basin region,
- Utah, Colorado and New Mexico: Chemical Geology, v. 4, no. 1-2, p. 263-294.
- 438 https://doi.org/10.1016/0009-2541(69)90050-3
- Haitjema, H. M., & Mitchell-Bruker, S. (2005). Are water tables a subdued replica of the topography?.
- 440 Groundwater, 43(6), 781-786.
- Hite R. J., Anders D. E., and Ging T. G., 1984, Organic-rich source rocks of Pennsylvanian age in the
- Paradox Basin of Utah and Colorado, in Woodward, J., Meissner F.F., and Clayton J.L., eds.,
- 443 Hydrocarbon Source Rocks of the Greater Rocky Mountain Region: Rocky Mountain Association of
- Geologists, Denver, Colorado, p. 255-274.
- Holland, G., Lollar, B. S., Li, L., Lacrampe-Couloume, G., Slater, G. F., & Ballentine, C. J. (2013). Deep
- fracture fluids isolated in the crust since the Precambrian era. Nature, 497(7449), 357-360.
- Jasechko, S., Perrone, D., Befus, K. M., Cardenas, M. B., Ferguson, G., Gleeson, T., ... & Kirchner, J. W.
- 448 (2017). Global aquifers dominated by fossil groundwaters but wells vulnerable to modern contamination.
- 449 Nature Geoscience, 10(6), 425-429.

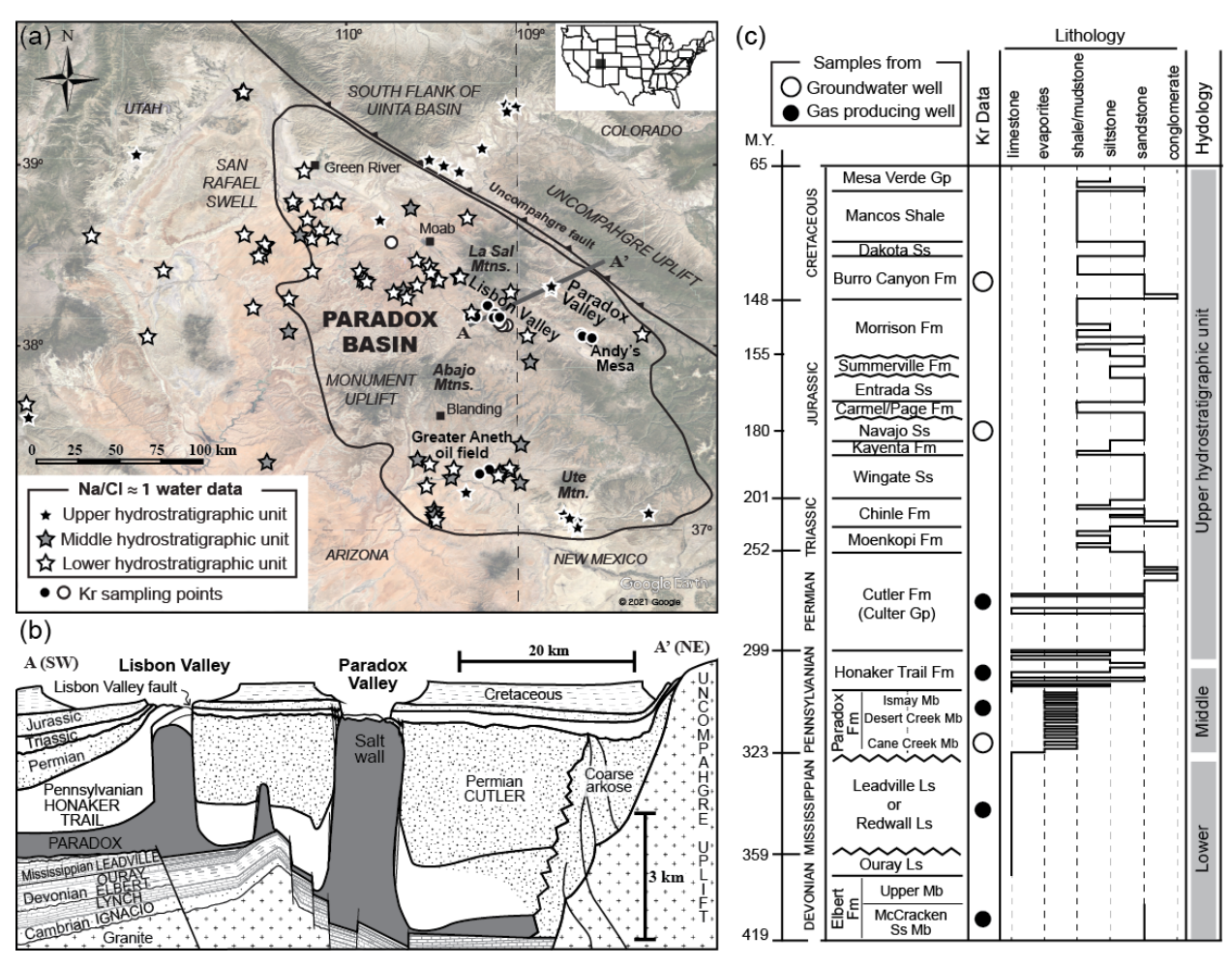
- 450 Jiang, W., Bailey, K., Lu, Z. T., Mueller, P., O'Connor, T. P., Cheng, C. F., ... & Yang, G. M. (2012). An
- atom counter for measuring 81Kr and 85Kr in environmental samples. Geochimica et Cosmochimica
- 452 Acta, 91, 1-6.
- Jiang, W., Hu, S. M., Lu, Z. T., Ritterbusch, F., & Yang, G. M. (2020). Latest development of
- radiokrypton dating—A tool to find and study paleogroundwater. Quaternary International, 547, 166-171.
- Kang, M., & Jackson, R. B. (2016). Salinity of deep groundwater in California: Water quantity, quality,
- and protection. Proceedings of the National Academy of Sciences, 113(28), 7768-7773.
- 457 Karlstrom, K. E., Coblentz, D., Dueker, K., Ouimet, W., Kirby, E., Van Wijk, J., ... & CREST Working
- 458 Group. (2012). Mantle-driven dynamic uplift of the Rocky Mountains and Colorado Plateau and its
- surface response: Toward a unified hypothesis. Lithosphere, 4(1), 3-22.
- 460 Kim, J. H., Bailey, L., Noyes, C., Tyne, R. L., Ballentine, C. J., Person, M., ... & McIntosh, J. (2022).
- 461 Hydrogeochemical evolution of formation waters responsible for sandstone bleaching and ore
- 462 mineralization in the Paradox Basin, Colorado Plateau, USA. GSA Bulletin. doi:
- 463 <u>https://doi.org/10.1130/B36078.1</u>
- King, V. M., Block, L. V., Yeck, W. L., Wood, C. K., & Derouin, S. A. (2014). Geological structure of
- the Paradox Valley Region, Colorado, and relationship to seismicity induced by deep well injection.
- Journal of Geophysical Research: Solid Earth, v. 119, no. 6, p. 4955-4978.
- Kharaka, Y. K. & Hanor, J. S. (2014). Deep fluids in sedimentary basins, in Turekian K. K. Holland H.
- D., eds., Treatise on Geochemistry, 2nd edition, Meteorites and Cosmochemical Processes, volume editor,
- 469 Andrew M. Davis. New York, Elsevier Ltd., Ch. 7, p. 471–515, section 7.14.4.6.
- 470 Lazear, G., Karlstrom, K., Aslan, A., & Kelley, S. (2013). Denudation and flexural isostatic response of
- the Colorado Plateau and southern Rocky Mountains region since 10 Ma. Geosphere, 9(4), 792-814.
- Lehmann, B. E., Love, A., Purtschert, R., Collon, P., Loosli, H. H., Kutschera, W., ... & Groening, M.
- 473 (2003). A comparison of groundwater dating with 81Kr, 36Cl and 4He in four wells of the Great Artesian
- Basin, Australia. Earth and Planetary Science Letters, 211(3-4), 237-250.
- 475 Lollar, B. S., Heuer, V. B., McDermott, J., Tille, S., Warr, O., Moran, J. J., ... & Hinrichs, K. U. (2021). A
- window into the abiotic carbon cycle–Acetate and formate in fracture waters in 2.7 billion year-old host
- 477 rocks of the Canadian Shield. Geochimica et Cosmochimica Acta, 294, 295-314.
- Loosli, H. H., & Oeschger, H. (1969). 37Ar and 81Kr in the atmosphere. Earth and Planetary Science
- 479 Letters, 7(1), 67-71.
- 480 Lu, Z. T., Schlosser, P., Smethie Jr, W. M., Sturchio, N. C., Fischer, T. P., Kennedy, B. M., ... &
- 481 Yokochi, R. (2014). Tracer applications of noble gas radionuclides in the geosciences. Earth-Science
- 482 Reviews, 138, 196-214.
- 483 Ma, L., Castro, M. C., & Hall, C. M. (2009). Crustal noble gases in deep brines as natural tracers of
- vertical transport processes in the Michigan Basin. Geochemistry, Geophysics, Geosystems, 10(6).
- 485 Matsumoto, T., Chen, Z., Wei, W., Yang, G. M., Hu, S. M., & Zhang, X. (2018). Application of
- 486 combined 81Kr and 4He chronometers to the dating of old groundwater in a tectonically active region of
- the North China Plain. Earth and Planetary Science Letters, 493, 208-217.

- Matsumoto, T., Zouari, K., Trabelsi, R., Hillegonds, D., Jiang, W., Lu, Z. T., ... & Agoun, A. (2020).
- 489 Krypton-81 dating of the deep Continental Intercalaire aquifer with implications for chlorine-36 dating.
- Earth and Planetary Science Letters, 535, 116120.
- 491 McIntosh, J. C., & Ferguson, G. (2021). Deep Meteoric Water Circulation in Earth's Crust. Geophysical
- 492 Research Letters, 48(5), e2020GL090461.
- Molenaar, C. M. (1981). Mesozoic stratigraphy of the Paradox Basin- An overview, in Wiegand, D.L.,
- ed., Geology of the Paradox Basin: Rocky Mountain Association of Geologists Guidebook, p. 119–127.
- 495 Murray, K. E., Reiners, P. W., Thomson, S. N., Robert, X., & Whipple, K. X. (2019). The
- thermochronologic record of erosion and magmatism in the Canyonlands region of the Colorado Plateau.
- 497 American journal of science, 319(5), 339-380.
- Neuzil, C. E. (1986). Groundwater flow in low-permeability environments. water resources research,
- 499 22(8), 1163-1195.
- Noyes, C., Kim, J., Person, M., Ma, L., Ferguson, G., & McIntosh, J. C. (2021). A geochemical and
- isotopic assessment of hydraulic connectivity of a stacked aquifer system in the Lisbon Valley, Utah
- 502 (USA), and critical evaluation of environmental tracers. Hydrogeology Journal, 1-19.
- 503 <u>https://doi.org/10.1007/s10040-021-02361-9</u>
- Nuccio, V. F., & Condon, S. M. (1996). Burial and thermal history of the Paradox Basin, Utah and
- 505 Colorado, and petroleum potential of the middle Pennsylvanian Paradox Formation.
- Pederson, J., Burnside, N., Shipton, Z., & Rittenour, T. (2013). Rapid river incision across an inactive
- fault—Implications for patterns of erosion and deformation in the central Colorado Plateau. Lithosphere,
- 508 5(5), 513-520.
- Person, M., McIntosh, J., Bense, V., & Remenda, V. H. (2007). Pleistocene hydrology of North America:
- The role of ice sheets in reorganizing groundwater flow systems. Reviews of Geophysics, 45(3).
- 511 Phillips, F. M. (2000). Chlorine-36. In Environmental tracers in subsurface hydrology (pp. 299-348).
- 512 Springer, Boston, MA.
- Ram, R., Purtschert, R., Adar, E. M., Bishof, M., Jiang, W., Lu, Z. T., ... & Burg, A. (2021). Controls on
- the 36Cl/Cl input ratio of paleo-groundwater in arid environments: New evidence from 81Kr/Kr data.
- Science of the Total Environment, 762, 144106.
- Sanford, R. F. (1994). A quantitative model of ground-water flow during formation of tabular sandstone
- uranium deposits. Economic Geology, 89(2), 341-360.
- 518 Schlegel, M. E., Zhou, Z., McIntosh, J. C., Ballentine, C. J., & Person, M. A. (2011). Constraining the
- timing of microbial methane generation in an organic-rich shale using noble gases, Illinois Basin, USA.
- 520 Chemical Geology, 287(1-2), 27-40.
- Scott, A. R., Kaiser, W. R., & Ayers Jr, W. B. (1994). Thermogenic and secondary biogenic gases, San
- 522 Juan Basin, Colorado and New Mexico—implications for coalbed gas producibility. AAPG bulletin,
- 523 78(8), 1186-1209.
- 524 Spangler, L. E., Naftz, D. L., & Peterman, Z. E. (1996). Hydrology, chemical quality, and
- 525 characterization of salinity in the Navajo aquifer in and near the Greater Aneth Oil Field, San Juan

- County, Utah (Vol. 96, No. 4155). US Department of the Interior, US Geological Survey.
- 527 https://doi.org/10.3133/wri964155
- 528 Stevenson, G. M., and Baars, D. L., 1986, The Paradox: A Pull-Apart Basin of Pennsylvanian Age, in
- 529 Peterson, J.E. ed., Palcotectonics and Sedimentation in the Rocky Mountain Region, United States:
- American Association of Petroleum Geologists Memoir, 41, p. 513-539.
- 531 Sturchio, N., Du, X., Purtschert, R., Lehmann, B., Sultan, M., Patterson, L., Lu, Z. T., Müller, P., Bigler,
- T., & Bailey, K. (2004). One million year old groundwater in the Sahara revealed by krypton-81 and
- chlorine-36. Geophysical Research Letters, 31(5).
- 534 Sturchio, N. C., Kuhlman, K. L., Yokochi, R., Probst, P. C., Jiang, W., Lu, Z. T., ... & Yang, G. M.
- 535 (2014). Krypton-81 in groundwater of the culebra dolomite near the waste isolation pilot plant, New
- Mexico. Journal of contaminant hydrology, 160, 12-20.
- Thackston J. W., McCulley B. L., and Preslo, L. M., 1981, Ground-water circulation in the western
- Paradox Basin, Utah: in Wiegand, D. L., ed., Geology of the Paradox basin: Rocky Mountain Association
- of Geologists Field Conference, p. 201-225
- 540 Tóth, J. (1999). Groundwater as a geologic agent: an overview of the causes, processes, and
- manifestations. Hydrogeology journal, 7(1), 1-14.
- Warr, O., Lollar, B. S., Fellowes, J., Sutcliffe, C. N., McDermott, J. M., Holland, G., ... & Ballentine, C.
- J. (2018). Tracing ancient hydrogeological fracture network age and compartmentalisation using noble
- gases. Geochimica et Cosmochimica Acta, 222, 340-362.
- Yager, R. M., McCoy, K. J., Voss, C. I., Sanford, W. E., & Winston, R. B. (2017). The role of uplift and
- erosion in the persistence of saline groundwater in the shallow subsurface. Geophysical Research Letters,
- 547 44(8), 3672-681.
- Yechieli, Y., Yokochi, R., Zilberbrand, M., Lu, Z. T., Purtschert, R., Sueltenfuss, J., ... & Burg, A.
- 549 (2019). Recent seawater intrusion into deep aquifer determined by the radioactive noble-gas isotopes
- 81Kr and 39Ar. Earth and planetary science letters, 507, 21-29.
- Yokochi, R. (2016). Recent developments on field gas extraction and sample preparation methods for
- radiokrypton dating of groundwater. Journal of Hydrology, 540, 368-378.
- Yokochi, R., Ram, R., Zappala, J.C., Jiang, W., Adar, E., Bernier, R., Burg, A., Dayan, U., Lu, Z.-T.,
- Mueller, P., Purtschert, R., Yechieli, Y., 2019. Radiokrypton unveils dual moisture sources of a deep
- desert aquifer. Proc. Natl. Acad. Sci. 116, 16222–16228.
- Zhang, Y., Gable, C. W., Zyvoloski, G. A., & Walter, L. M. (2009). Hydrogeochemistry and gas
- compositions of the Uinta Basin: A regional-scale overview. AAPG bulletin, 93(8), 1087-1118.
- Zheng, L., Apps, J. A., Spycher, N., Birkholzer, J. T., Kharaka, Y. K., Thordsen, J., ... & Trautz, R. C.
- 559 (2012). Geochemical modeling of changes in shallow groundwater chemistry observed during the MSU-
- ZERT CO2 injection experiment. International journal of greenhouse gas control, 7, 202-217.
- Zhou, Z., Ballentine, C. J., Kipfer, R., Schoell, M., & Thibodeaux, S. (2005). Noble gas tracing of
- 562 groundwater/coalbed methane interaction in the San Juan Basin, USA. Geochimica et Cosmochimica
- 563 Acta, 69(23), 5413-5428.

565 Figure captions Figure 1. (a) Location of the Paradox Basin and spatial distribution of dissolution of evaporite (Na/Cl 566 567 ~1). (b) Schematic cross section of A-A' in (a) across the Paradox Basin, modified from Baars (1966), Stevenson and Baars (1986), and King et al. (2014). (c) Stratigraphic column with sample formation, 568 569 lithology, and hydrostratigraphic unit (Hanshaw and Hill, 1969). 570 Figure 2. (a) Corrected ⁸¹Kr abundance (pMKr) as a function of different geologic formations. Detectable 571 ⁸¹Kr abundance ranges from 3 to 100 pMKr (grey area). (b) δD_{water} values of formation waters showing a 572 binary mixing relationship between meteoric water and evaporated paleo-seawater (EPS) components. 573 574 High Cl/Br of formation waters indicates salt dissolution by influx of meteoric water. (c) Corrected ⁸¹Kr abundance of fluids versus corresponding δD_{water} values of formation waters. The estimated ⁸¹Kr age of 575 the meteoric water component of formation waters was calculated using δD_{water} values. 576 577 578 Figure 3. Schematic diagrams (a-b) of evolution of meteoric circulation in response to changes in the 579 equivalent freshwater head gradient (∇h) and topographical gradient (∇E) of an aquifer by erosion and 580 incision over geologic time, prior to denudation of the Colorado Plateau (a) and following erosion of the 581 Mancos Shale and incision of river outlets (b). Blue arrows represent fresh groundwater flow, while red 582 arrows represent saline fluid migration. Length of arrows represent magnitude of flow. (c) Comparison of DFR values for each formation based on before 10 Ma and modern topography. The color of the symbol 583 584 is identical to Figure 2.

Figure 1





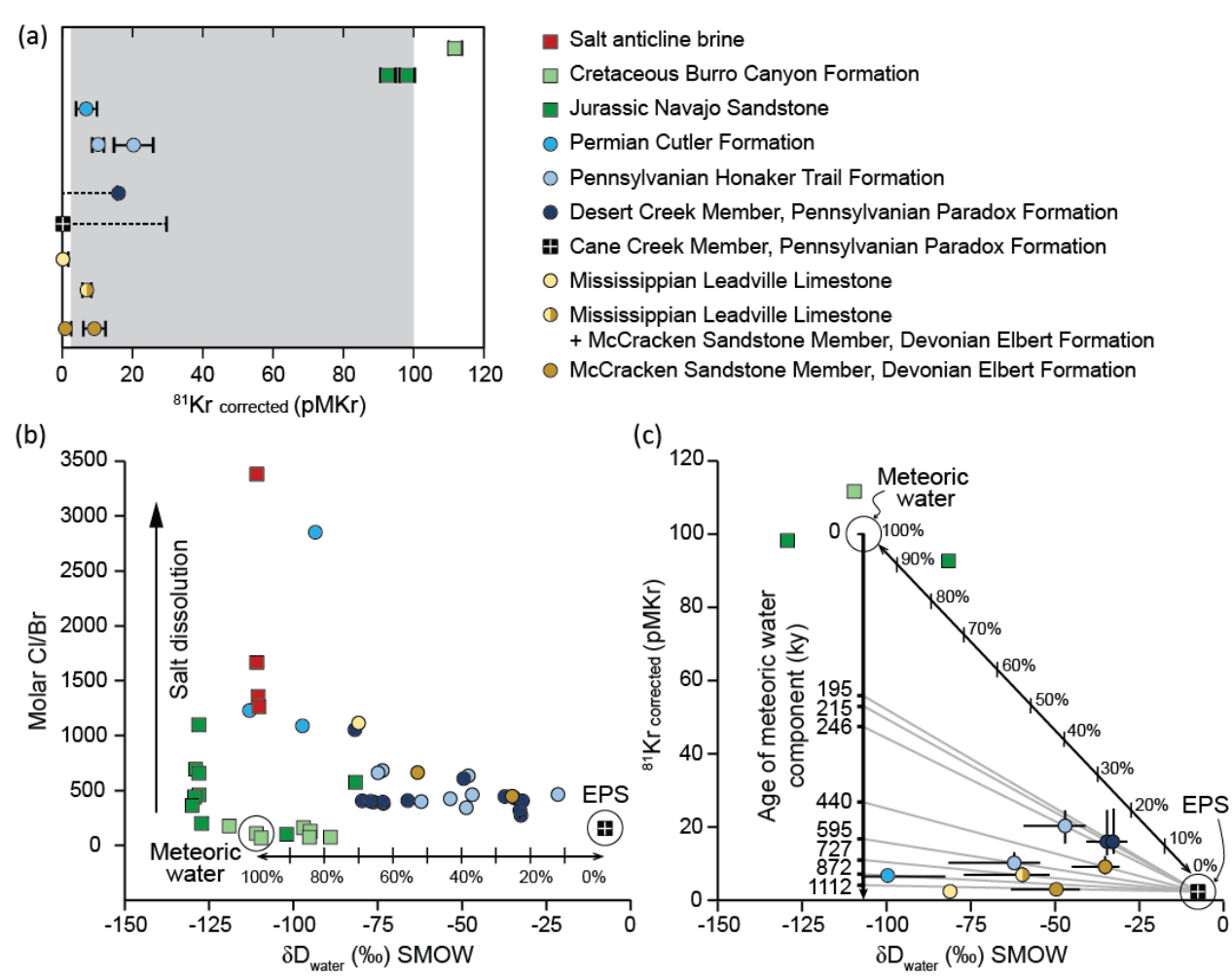
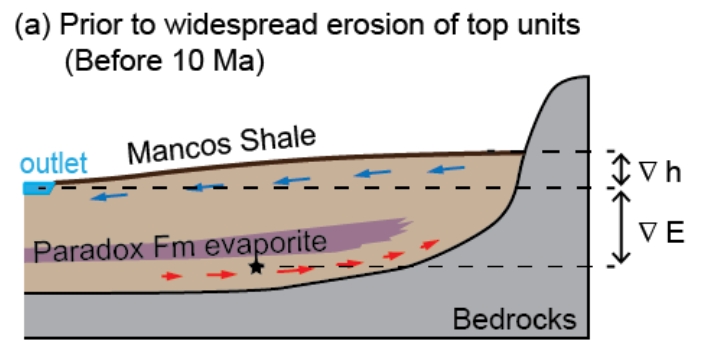
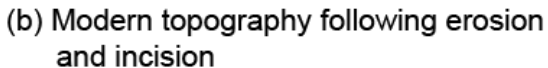
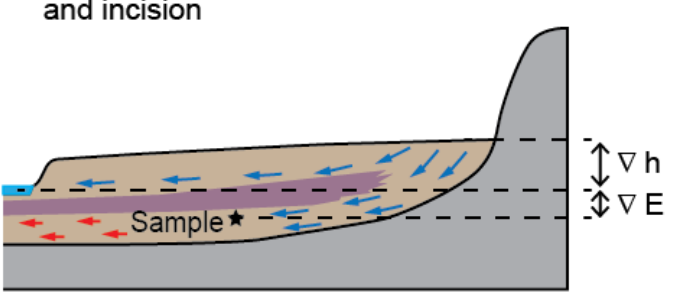
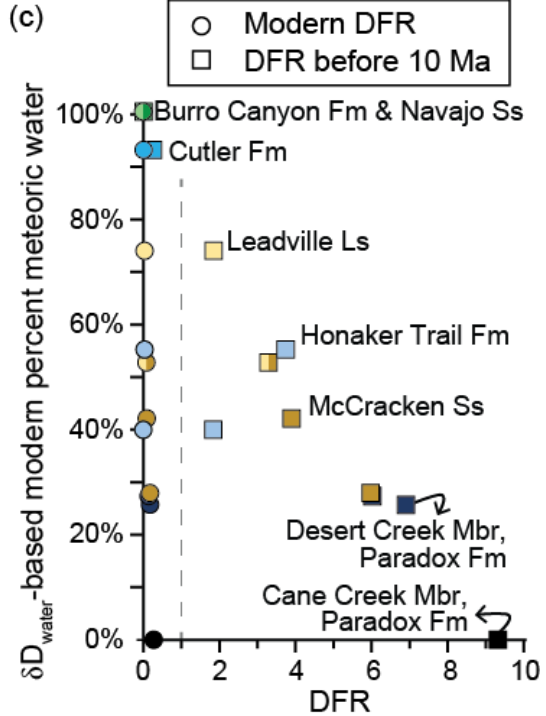


Figure 3











Geophysical Research Letters

Supporting information for

Krypton-81 dating constrains timing of deep groundwater flow activation

Ji-Hyun Kim¹, Grant Ferguson^{1,2}, Mark Person³, Wei Jiang⁴, Zheng-Tian Lu⁴, Florian Ritterbusch⁴, Guo-Min Yang⁴, Rebecca Tyne^{5*}, Lydia Bailey⁶, Chris Ballentine⁵, Peter Reiners⁶, Jennifer McIntosh^{1,2}

Department of Hydrology and Atmospheric Sciences, University of Arizona, Tucson, AZ, USA
 Department of Civil, Geological and Environmental Engineering, University of Saskatchewan, Saskatoon, Canada
 Department of Earth and Environmental Science, New Mexico Tech, Socorro, NM, USA
 School of Physics, University of Science and Technology of China, Hefei, China
 Department of Earth Sciences, University of Oxford, Oxford, England, UK
 Department of Geosciences, University of Arizona, Tucson, AZ, USA

* Rebecca Tyne is now affiliated with the Woods Hole Oceanographic Institution.

Contents of this file

- Table S1. Location and geologic formation of ⁸¹Kr samples
- Table S2. Analytical results of ⁸¹Kr and ⁸⁵Kr for dissolved/produced gas samples and hydrochemical data of water samples from corresponding wells or geologic formations
- Text S1. Detailed description of ⁸¹Kr sampling and purification/analysis procedures
- Figure S1. Groundwater degassing device based on membrane contactor developed at University of Science and Technology of China

Introduction

This supporting information provides the tables and the detailed methods as presented in the main article

Table S1. Location and geologic formation of ⁸¹Kr samples

Gas sample ID	Location	Latitude	Longitude	Depth (m)	Period	Formation
PW-12b	Lisbon Valley	38.1246	-109.1209	305	Cretaceous	Burro Canyon Formation (Fm)
PW-8b	Lisbon Valley	38.1478	-109.1345	472	Jurassic	Navajo Sandstone
PW-11b	Lisbon Valley	38.1262	-109.1007	457	Jurassic	Navajo Sandstone
AM-62	Andy's Mesa	38.0305	-108.2685	1711	Permian	Cutler Formation
MM 31-42	Lisbon Valley	38.2318	-109.2099	1613	Pennsylvanian	Honaker Trail Fm
MM 31-31	Lisbon Valley	38.2362	-109.2153	1522	Pennsylvanian	Honaker Trail Fm
Sahgzie 1	Greater Aneth	37.1696	-109.3064	1954	Pennsylvanian	Desert Creek members, Paradox Fm
Monument-8n-2	Greater Aneth	37.3163	-109.1979	1895	Pennsylvanian	Desert Creek members, Paradox Fm
Cane Creek 32	NW of Moab	38.5803	-109.7356	2239	Pennsylvanian	Cane Creek member, Paradox Fm
Lisbon B6-10	Lisbon Valley	38.1980	-109.2773	2369	Mississippian	Leadville Limestone
Lisbon D8-10	Lisbon Valley	38.1902	-109.2687	2441	Mississippian- Devonian	Leadville Limestone - McCracken Sandstone member, Elbert Fm
Lisbon D6-10	Lisbon Valley	38.1981	-109.2695	2370	Devonian	McCracken Sandstone member, Elbert Fm
Lisbon 10-33	Lisbon Valley	38.1915	-109.2737	2702	Devonian	McCracken Sandstone member, Elbert Fm

Table S2. Analytical results of ⁸¹Kr and ⁸⁵Kr for dissolved/produced gas samples and hydrochemical

data of water samples from corresponding wells or geologic formations

Gas sample ID	⁸⁵ Kr activity (dpm/cc)	⁸¹ Kr (pMKr)	⁸¹ Kr _{corrected} (pMKr) ^a	⁸¹ Kr age (ka)	Cl/Br	TDS (g/L)	δ ¹⁸ O _{water} (‰, SMOW)	δD _{water} (‰, SMOW)
PW-12b	4.65 ± 0.4	111.7 ± 2.3	112.5 ± 2.5	Anomaly	73	1.26	-14.66	-109.51
PW-8b	1.04 ± 0.1	92.7 ± 2.5	92.5 ± 2.5	$25.8^{+9.7}_{-9.4}$	576	0.88	-12.23	-81.61
PW-11b	1.84 ± 0.2	98.2 ± 2.5	98.2 ± 2.6	<23	441	0.70	-17.28	-129.35
AM-62	1.95 ± 0.7	9.4 ± 3.0	6.8 ± 3.2	890^{+210}_{-130}	1725 ^d	11.4 ^d	-12.78 ^d	-99.60 ^d
MM 31-42	10.3 ± 2.1	32.0 ± 4.4	20.3 ± 5.9	530^{+110}_{-80}	463	82.8	-4.48	-46.99
MM 31-31	<1.2	10.2 ± 2.0	C.N.N.c	754^{+72}_{-59}	401	171	-5.23	-62.11
Sahgzie 1	23.8 ± 1.5	37.8 ± 3.2	<16	>600	320	255	4.93	-32.88
Monument-8n-2	< 5.1	<16	C.N.N.	>600	436	234	4.96	-34.57
Cane Creek 32	58.8 ± 1.7	84.0 ± 3.1	0.7 ± 28.1	Too uncertain	156	334	4.98	-7.57
Lisbon B6-10	<1.4	< 2.5	C.N.N.	>1200	1115e	70.3 e	-8.20 e	-80.65 e
Lisbon D8-10	1.5 ± 0.4	9 ± 1.3	7 ± 1.4	878^{+74}_{-60}	743 ^f	123 ^f	-0.98 ^f	-59.64 ^f
Lisbon D6-10	7.9 ± 0.6	10.2 ± 2.1	< 2.9	>1200	557 g	150 g	2.64 g	-49.14 ^g
Lisbon 10-33	2.9 ± 1.0	12.9 ± 3.1	9.1 ± 3.5	790^{+160}_{-110}	449	212	0.91	-35.12
Air-1 ^b	70.1 ± 1.9	105.9 ± 4.4	C.N.N.	= .	-	-	=	-

^{a 81}Kr corrected for modern air

Note: Comparisons of 81Kr data with hydrochemical data is based on the assumption of homogeneity of fluid age and hydrochemistry across the same aquifer systems or large formations and across gas and water phase partitions.

^b The air sample was collected in Aug. 2018 and measured in June 2019.

^c C.N.N.: Correction not needed

^d Averaged data from Greater Aneth oil field; Spangler et al. (1996)

^e Data from Lisbon Valley: McIntyre 17-21; Kim et al. (2022)

f Averaged data from Lisbon Valley: McIntyre 17-21; Lisbon B8-10; Lisbon 10-33; Kim et al. (2022)

g Averaged data from Lisbon Valley: Lisbon B8-10; Lisbon 10-33; Kim et al. (2022)

Text S1. Detailed description of ⁸¹Kr sampling and purification/analysis procedures

Sampling Procedure

A gas extraction device is a portable sampling device built by our co-authors to extract dissolved gas from groundwater using a semi-permeable membrane and vacuum pump (Jiang et al., 2020). The device was connected between a wellhead and an aluminum gas tank and used to evacuate the gas tanks and connector pipes between the wellhead and the gas tanks using the vacuum pump before sampling to prevent air contamination.

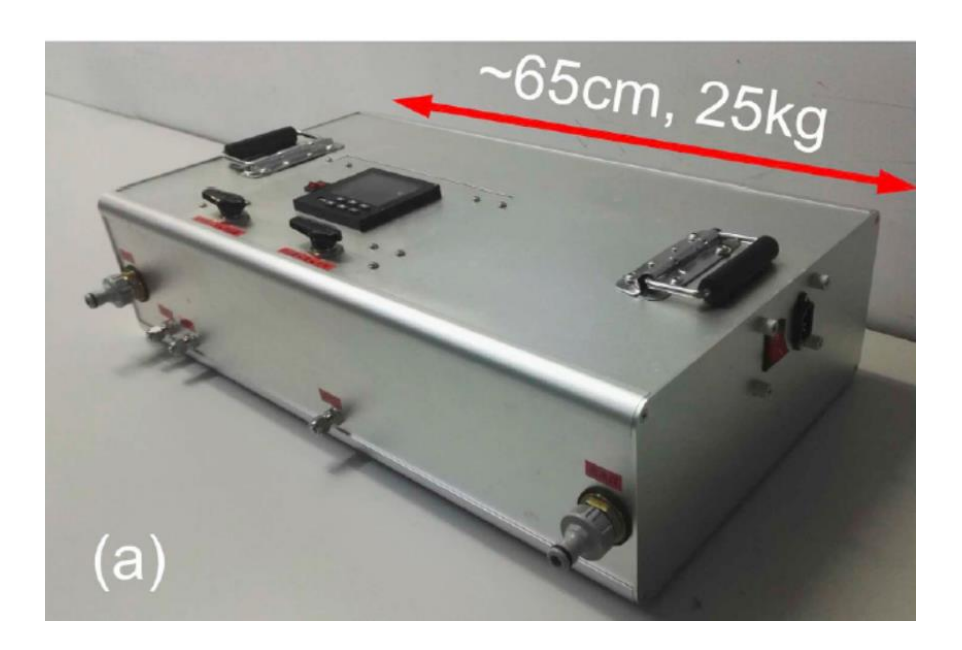


Figure S1. Groundwater degassing device based on membrane contactor developed at University of Science and Technology of China (Jiang et al., 2020)

In the case of oil and gas producing wells, the gas samples were collected into aluminum gas tanks attached to the gas producing wellhead through a pressure regulator. In case of groundwater wells, a hydrophobic membrane in the device was used to extract dissolved gas from water and convey the extracted gas to evacuated gas tanks (Yokochi, 2016; Jiang et al., 2020).

The krypton age tells us how long the gas has been isolated from the modern air. The fractionation of krypton in the gas phase and water depends on how the krypton gas entered the water but should be very small compared to the measurement uncertainty. Therefore, we assumed the fractionation effect is

negligible so that we can use the krypton age to estimate the groundwater residence time in assumption that (1) krypton gas in air was carried by the groundwater when the groundwater recharged, (2) the krypton gas contacted with formation fluids (oil, gas, and residual brines) in subsurface, and (3) there is no source of Kr from the subsurface.

Purification/Analysis Procedures

Kr separation from the gases and the ⁸¹Kr analysis were performed at the University of Science and Technology of China (USTC). An automated Kr purification system capable of handling methane-rich gases was used for the Kr separation (Dong et al., 2019). Processing gas samples with high methane contents is a challenging task. The Kr separation and purification was done at USTC with a home-build Kr purification system. This system is capable of handling methane-rich gas samples (up to 95%, X.-Z. Dong et al., Dual Separation of Krypton and Argon from Environmental Samples for Radioisotope Dating, Anal. Chem. 91, 21, 13576 (2019)). The key is a dual-temperature zone Ti-oven, which can break down methane and absorb it efficiently. After the methane and most of the active gases are removed by the Ti-oven, the remaining gas is sent to a GC for Kr separation. A getter pump is used to remove the trace amount of active gases from the Kr sample before final collection. The Atom Trap Trace Analysis (ATTA) method was used for the ⁸¹Kr analysis (Jiang et al., 2012 & 2020).

Reference

Dong, X. Z., Ritterbusch, F., Chu, Y. Q., Gu, J. Q., Hu, S. M., Jiang, W., ... & Zhao, L. (2019). Dual separation of krypton and argon from environmental samples for radioisotope dating. Analytical chemistry, 91(21), 13576-13581.

Jiang, W., Bailey, K., Lu, Z. T., Mueller, P., O'Connor, T. P., Cheng, C. F., ... & Yang, G. M. (2012). An atom counter for measuring 81Kr and 85Kr in environmental samples. Geochimica et Cosmochimica Acta, 91, 1-6.

Jiang, W., Hu, S. M., Lu, Z. T., Ritterbusch, F., & Yang, G. M. (2020). Latest development of radiokrypton dating—A tool to find and study paleogroundwater. Quaternary International, 547, 166-171.

Yokochi, R. (2016). Recent developments on field gas extraction and sample preparation methods for radiokrypton dating of groundwater. Journal of Hydrology, 540, 368-378.